IEEE Access
Multidisciplinary | Rapid Review | Open Access Journal

Received July 25, 2019, accepted August 22, 2019, date of publication August 26, 2019, date of current version September 30, 2019.

Digital Object Identifier 10.1109/ACCESS.2019.2937636

Detection and Characterization Method for Interface Bonding Defects of New Composite Materials

YINTANG WEN, SONG ZHANG, AND YUYAN ZHANG
School of Electrical Engineering, Yanshan University, Qinhuangdao 066004, China
Key Laboratory of Measuring and Testing Technologies and Instrumentation of Hebei Province, Yanshan University, Qinhuangdao 066004, China

Corresponding author: Yuyan Zhang (yyzhang@ysu.edu.cn)

This work was supported by the Provincial Natural Science Foundation of Hebei under Grant E2017203240.

ABSTRACT The defects such as voids and debonding within the bonding interface between the composite and the substrate are the key factors affecting the safe use of materials. In this study, Industrial Computed Tomography (ICT) was used to perform non-destructive tests of bonding defects. High-precision characterization methods are required to quantify the defects. This paper proposes an improved image segmentation processing method for accurate extraction of defect edges and quantitative characterization. With the proposed method combining mathematical morphology and Fuzzy C-Means (FCM) threshold segmentation, the irregular defects of voids and debonding can be visualized and established with corresponding quantitative indicators. The experimental results show that the defect area error of the tested bonding layer is within $\pm 6\%$, which satisfies the requirements of accurate detection and characterization of interface bonding layer defects of composite components. This work provides a strong technical basis for the reliability assessment of new ceramic matrix composites (CMCs) bonded structural members.

INDEX TERMS Interface bonding defects, voids and debonding, industrial computed tomography (ICT), segmentation method, detection and characterization.

I. INTRODUCTION

New Ceramic matrix composites (CMCs) are in demand in aerospace industry [1], [2] due to excellent properties such as low density, thermal insulation and sound insulation [3]–[7]. When the CMCs is used as a protective material, it is bonded to the substrate of the protected object. In the process of bonding, even after extensive research and experimentation to establish a reasonable manufacturing process, the existence of defects is inevitable, thereby leading to serious damage to the life, reliability, functionality and safety of the structure. In order to avoid the interface defects of composite bonding layer such as viscous, debonding and voids, it is necessary to introduce Non-destructive testing and evaluation methods.

The anisotropy and heterogeneity of new CMCs pose great challenges for measurement and calculation. At present, the existing non-destructive testing technologies mainly include eddy current, ultrasonic method, infrared thermal wave method and laser speckle imaging detection methods [8]–[15], but there is no common technology for non-destructive testing and evaluation of ceramic matrix composite materials. According to the structural anisotropism of new CMCs, traditional detection methods such as eddy current, ultrasonic, and infrared thermal imaging are limited by a certain degree of application. Ultrasonic method has a large attenuation in the strongly absorbing composite material, and the ultrasonic signal at the deep interface is weak. So the ultrasonic method has poor applicability to the detection of internal defects of thick composite materials; The low-frequency eddy current technology must first confirm the internal structure of the composite material to determine its detection method; Infrared thermal wave detection is suitable for the detection of composite thin plates and is sensitive to the ambient temperature. Consequently, it is difficult to be sensitive to the adhesive layer through the high heat insulation and heat protection structure. Therefore, it is very urgent and important to study the

The associate editor coordinating the review of this article and approving it for publication was Chao Tan.

detection technology and method suitable for new materials to realize the detection and visual characterization of material bonding defects.

ICT (Industrial Computed Tomography) technology [16]–[18], with high-quality density resolution and spatial resolution, can give two-dimensional or three-dimensional reconstruction images of the detected workpiece [19]. Compared with other technologies such as scanning electron microscopy, ICT technology can deeply analyze the internal structure without damaging the material structure.

Lall *et al.* [20] proposed a two-dimensional grayscale image of a measured object by using a monochromatic light to focus a rotating object in a ray field. Under the ICT non-destructive testing method, a complex reconstruction algorithm is used to reconstruct the three-dimensional internal image, and defects such as cracks and holes are detected. Perrier *et al.* [21] used micro-CT to study the effects of water aging on the damage caused by woven fiber/epoxy composites and the tensile load of the material itself, and effectively quantify the deformation and damage inside the specimen. Li *et al.* [22] studied the fracture modes of fiber fracture, debonding, resin cracking and interlayer delamination caused by three-dimensional braided composites under impact shear loading using micro-CT and interface geometry model based on woven preformed structure. Mehdikhani *et al.* [23] used X-ray micro-computer tomography to segment and quantitatively analyze the pores in different stacking order carbon/epoxy laminates. The shape, size parameters, orientation and spatial distribution characteristics of the holes are obtained. Xue *et al.* [24] studied the feasibility of X-ray CT to explore the correlation between the intensity and mesostructure of CTMC. However, in the academic field, ICT technology mostly deals with the detection of defects in the base material, and the research results on the adhesive layer defects of the composite structure are very rare. Therefore, this paper proposes that it is necessary to study the defects such as debonding, viscous and voids of the new CMCs bonding layer based on ICT.

Some studies [24]–[28] used FCM segmentation algorithm to quantitatively analyze CT tomographic image defects. From the perspective of CT image segmentation and extraction of defects, these studies have still a few shortcomings on accurate quantitative calculations; As a consequence, the FCM algorithm alone hardly achieves the target requirements. Therefore, the appropriate segmentation method is crucial for the quantitative analysis of the composite interface bonding defect and the performance test of materials.

In this study, according to the characteristics and detection needs of the new ceramic matrix composite materials, based on the industrial CT detection principle, the research method of combining mathematical morphology with FCM threshold segmentation is proposed. In order to accurately realize the characterization of defects in the bonding, the comparison between published segmentation algorithm and proposed method in this study shows that the method developed in this paper is reasonable. The quantitative information

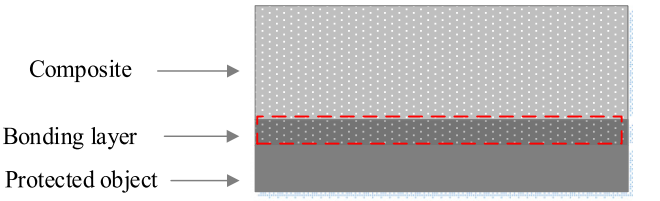

FIGURE 1. Structure of CMCs specimen.

such as quantity, area proportion and distribution are given, which provides the basis for further evaluation of the bonding quality of the components.

II. SPECIMEN AND METHODS

A. DESCRIIPTION OF CMCS SPECIMEN

The specimen of this paper is represented in Fig1. The structure of the specimen consists of three layers, respectively composite layer, bonding layer and protected object. Then the main components of specimen are O, Si and a small amount of Al. Therefore, the main material of the dendritic fiber of the composite material is SiO_2, that is, glass fiber; The ceramic matrix composite material is formed by cross-linking and sintering of dendritic inorganic fibers. The cross-linking between fibers is relatively dense and has a certain orientation in the cross-section, so the material exhibits obvious anisotropy feature. During the manufacturing process, the bonding layer of composite material and the substrate is prone to defects, resulting in material failure. Therefore, this paper investigates the defects such as interfacial debonding and void of the Fig1 red box bonding layer CMCs.

B. X-RAY COMPUTED TOMOGRAPHY TESTS

The equipment used in this experiment was an X-ray three-dimensional computed tomography system. The scanning facility of ICT is shown in Fig2. The detection technology includes two processes of data collection and data processing. First, the X-ray source is used to illuminate the sample while imaging it with a detector; Then, a series of projection data is generated by computer software, and FDK reconstruction algorithm is processed based on the X-ray attenuation coefficient of each component in the sample to reconstruct the 2D image and 3D image; Finally, the reconstructed 3D image and 2D slice image are processed by the complex software that ICT comes with. The system uses a cone beam X-ray source to scan structural images at 1μm resolution. ICT is a non-destructive testing method for visualizing materials and generating complete 3D images. It relies on a computer reconstruction algorithm to reconstruct the projection data acquired at different angles by rotating the specimen. The spatial distribution of the absorption coefficient is used to reconstruct a 3D volume image of the sample. Reconstruction of this paper involved steps, which we have described in red square of Fig3.

There are several artificially designed defects on the bonding layer of the composite material. In order to analyze the defect information of the bonding layer,

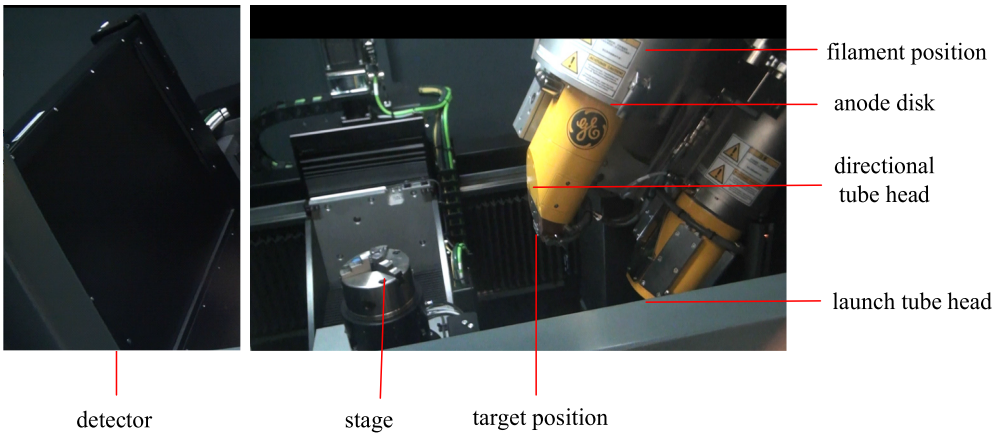

FIGURE 2. View of the CT experimental facility.

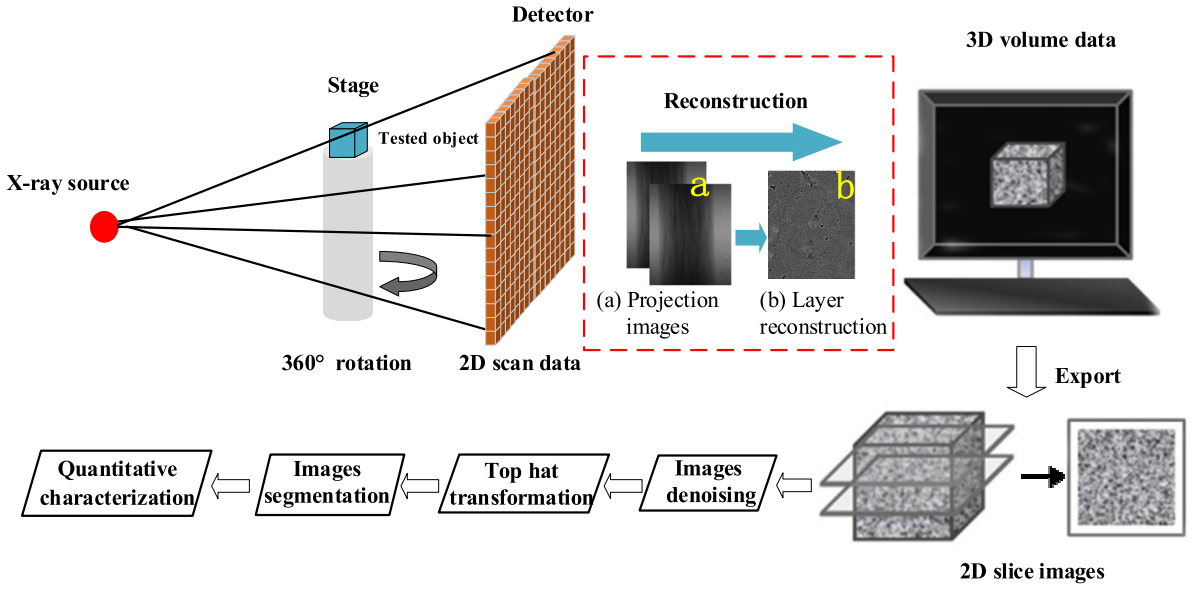

FIGURE 3. CT image-processing procedure.

the three-dimensional volume data is layered into a number of two-dimensional image sequences of 2014 × 1024 size according to the Z-axis.

III. METHOD FOR ICT DATA ANALYSIS

The data processing procedure presented in this paper is shown in Fig3. Firstly, the original ICT projection image is reconstructed and the three-dimensional tomographic image is obtained. Then the 3D image is divided into several 2D CT slice image. In order to accurately quantify the interface defects of the adhesive layer, the mathematical morphology and FCM segmentation method are used to extract the defects. Finally, the area and volume of the defects are quantitatively calculated.

A. SEGMENTATION ALGORITHM BASED ON ICT IMAGES

1) PRETREATMENT

The layered image of the composite bonding layer has the characteristics of low gray scale contrast, blurred edges, and many noise information, so the defect features may be submerged. In order to reduce the influence of noise and other factors, the average filtering of 5 × 5 template is performed on the two-dimensional image sequence.

2) LAYER IMAGE DEFECT SRGMENTATION AND EXTRACTION

a: MORPHOLOGICAL FILTERING

The image generally includes information such as: target information, background information and noise; The target information needs to be extracted, and background information and noise of influence the extraction of target information are useless information. Although the layered image of the CMCs is filtered by the mean value, there is still a lot of noise. The background and noise of the image are the main factors affecting the image segmentation effect. If the background and noise of the image can be reduced or even eliminated, the image segmentation effect will be improved a lot. According to the mathematical morphology principle, using a structural element of a certain size, it is possible to

shield a target larger than the size of the element by using a top hat transformation. Morphological image segmentation is a series of mathematical calculations by applying different structural elements to the original image. Therefore, the difference in size and shape of the structural elements will have a series of effects on the segmentation. To this end, the experiment uses a rectangular structure operator of 5×5 to perform a top hat transformation on the image to enhance the defective portion of the image. The principle is:

The function $g(x)$ is defined as a structure function whose symmetric function is represented by $g_s(x)$, namely:

$$g_s(x) = g(-x)$$

Then the function $f(x)$ is a definition of grayscale expansion and corrosion of $g(x)$, where,

$$\text{expansion} : [f \oplus g_s](x) = \max_{z \in D, z-x \in G} (f(z) + g(z-x))$$
$$\text{corrosion} : [f \Theta g_s](x) = \max_{z \in D, z-x \in G} (f(z) - g(z-x))$$

Let F_{G1} and F_{G2} respectively represent the results of the opening and closing operations of the function $f(x)$.The opening and closing operations are composed of expansion and corrosion, which are defined as follows.

$$\text{opening} : F_{G1} = [f \Theta g_s \oplus g](x)$$
$$\text{closing} : F_{G2} = [f \oplus g_s \Theta g](x)$$

Combine with 4 basic operations, you can generate some new operations, and the segmentation effect is better.

b: FCM THRESHOLD SEGMENTATION

FCM algorithm is a commonly used segmentation method. When the image contrast is high and it is not contaminated by noise, the FCM algorithm can achieve a better segmentation effect better than other segmentation methods. However, for the uneven background brightness of the interface bonding defect slice, the boundary contour of the defect region is blurred, which has a certain influence on the quantitative characterization of defects. To this end, in view of the problem of poor segmentation effect of FCM algorithm, this study proposes the improved algorithm of combining the top hat transform in morphology with FCM algorithm to obtain the image with slice background equalization, so that the defect segmentation effect map is brighter than the area around the original image contour.

The FCM algorithm achieves continuous optimization of the objective function (intra-class error squared sum function) through iterative operation. The application of image segmentation is based on the weighted membership degree between each center of the pixel and c cluster centers in the image. The iterative optimization is performed multiple times to obtain the clustering center matrix ·P and the fuzzy partition matrix ·U when the cluster objective function ·J is the smallest.

In the fuzzy c-means clustering algorithm, u_{ij} represents that the j sample belongs to the membership degree of the i cluster, and U is composed of u_{ij};

$$\sum_{i}^{c} u_{ij} = 1 \tag{1}$$

The clustering objective function J is:

$$\mathrm{J} = \sum_{i=1}^{c}\sum_{j=1}^{n} u_{ij}^{m} d_{ij}^{2} = \sum_{i=1}^{c}\sum_{j=1}^{n} u_{ij}^{m} \,||\, p_i - x_j \,||^2 \tag{2}$$

where: n is the total number of pixels in the image; m is the weighted index, which determines the degree of classification blur; $||\, p_i - x_j \,||^2$ is the Euclidean distance between the sample x_j and the cluster center p_i, and all p1 constitutes P. For the constraint $\sum_i^c u_{ij} = 1$, the Lagrange multiplier λ is introduced, and the clustering objective function can be written as

$$\mathrm{J} = \sum_{i=1}^{c} d_{ij}^{2} + \lambda \left(1 - \sum_{i=1}^{c} u_{ij}\right) \tag{3}$$

In order to obtain the fuzzy partition matrix U when the clustering objective function J is the smallest, the partial derivative of λ and u_{ij} is obtained for the objective function, so that it is 0, then there is

$$\frac{\partial J}{\partial \lambda} = 1 - \sum_{i=1}^{c} u_{ij} = 0 \tag{4}$$

$$\frac{\partial J}{\partial u_{ij}} = m \cdot u_{ij}^{m-1} \cdot d_{ij}^{2} - \lambda = 0 \tag{5}$$

From formula (4) and formula (5):

$$u_{ij} = \frac{1}{\sum_{k=1}^{c} \left(\frac{1}{d_{kj}^{2}}\right)^{\frac{1}{m-1}}} \cdot \left(\frac{1}{d_{ij}^{2}}\right)^{\frac{1}{m-1}} = \frac{1}{\sum_{k=1}^{c} \left(\frac{d_{ij}^{2}}{d_{kj}^{2}}\right)^{\frac{1}{m-1}}} \tag{6}$$

If the partial derivative of the objective function with respect to the clustering center p_i is 0, then there is:

$$\frac{\partial J}{\partial p_i} = \frac{\partial}{\partial p_i} \sum_{i=1}^{c}\sum_{j=1}^{n} u_{ij}^{m} \,||\, p_i - x_j \,||^2 = 0 \tag{7}$$

Finally, you can get the update formula for p_i:

$$p_i = \frac{\sum_{j=1}^{n} u_{ij}^{m} x_j}{\sum_{j=1}^{n} u_{ij}^{m}} \tag{8}$$

Thus, to provide a solid theoretical basis for the accurate analysis of interface defects of composites, the method above can be applied to directly measure and extract interface defects of testing sample.

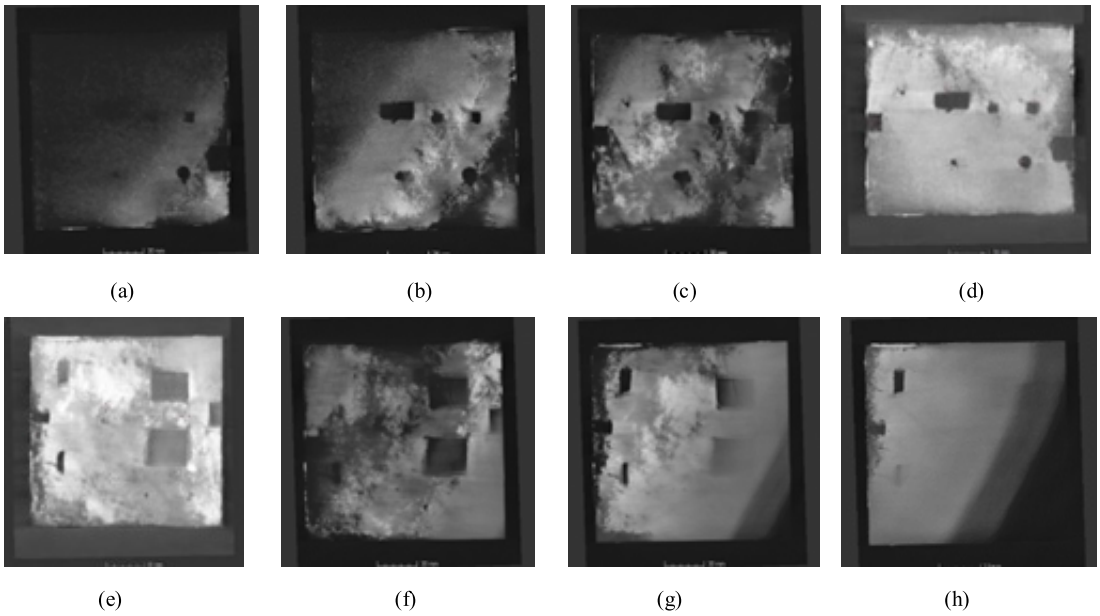

FIGURE 4. ICT images of bonding layer slice.

TABLE 1. Parameters of the scanning CT of the composites.

Voltage(kV)	Current（μA）	Angle(°)	Exposure time(ms)	Resolution(μm)	Width(pixels)	Height(pixels)
160	140	0.18	500	1	2014	1024

TABLE 2. Proportional size of the defect 30 mm=0.4(1 mm=0.013).

	A	B	C	D	E	F
length	0.10	0.18	0.07	0.39	0.40	0.14
width	0.24	0.10	0.20	0.32	0.38	0.26

IV. RESULTS AND DISCUSSION

The bonding layer of composites specimen is prefabricated voids and debonding defects. Based on the principle of industrial CT, after the sample is scanned by ICT system 360° rotation, a total of 2000 images were obtained. The following two types of defects are analyzed as follows.

A. DETECTION OF VOID DEFECTS IN COMPOSITE BONDING LAYER

In this paper, a sample of ceramic matrix composite material prefabricated void defects in the bonding layer was selected to quantify the indicators of defects and validate the effectiveness of the proposed method. Under the scanning of ICT technology, the scanning parameters are shown in Table 1. The void defects number, position, and type of each layer were observed by layer for the side view of the bonding layer of the sample. The CT scan slice images at the bonding layer are exhibited in Fig4.

In order to accurately calculate the size of the void defects, Fig5 is a void defect diagram selected in the interface diagram of several bonding layers. The bonding layer slice diagram is displayed at Fig5(a), including front view, side view, top view, 3D map. There are 6 adhesive layer defects in the top view of the defect distribution, which are A, B, C, D, E, F (as marked in Fig5(b)); The proportional dimensions and actual dimensions of the hole defects of A, B, C, D, E, and F are given in Tables 2 and 3, respectively. According to the results of the defect slice diagram analysis, based on the conditions of the ICT system, the area and type of void defects can be clearly obtained.

B. DETECTION OF DEBONDING DEFECTS IN COMPOSITE BONDING LAYER

Artificially prefabricating cross-channel debonding defects at the interface of the bonding layer, after the scanning of the industrial CT system is completed, Fig6 shows the cross-channel two-dimensional defect map. Through the analysis of the two-dimensional tomographic image, we can judge whether there is a defect in the bonding layer. And then the position, shape and other information of debonding defects can be observed.

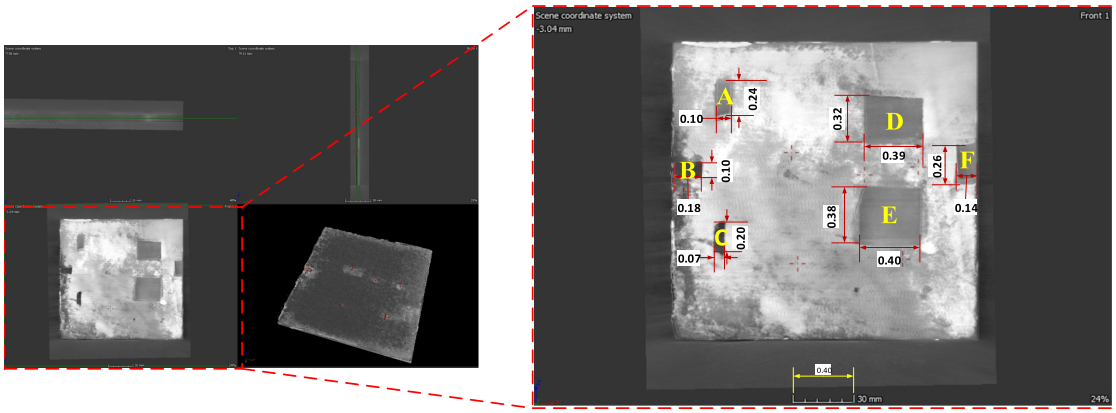

(a) (b)

FIGURE 5. Holes defect in slices.

TABLE 3. Actual size of the defect/mm.

	A	B	C	D	E	F
length	7.52	13.53	5.26	29.32	30.08	10.53
width	18.05	7.52	15.04	24.06	28.57	19.55

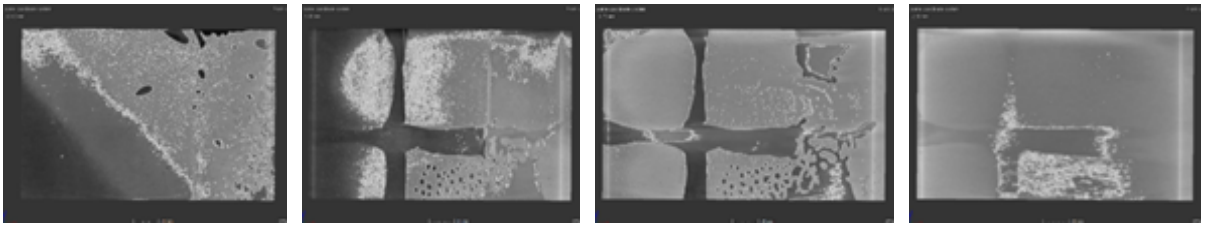

(a) (b) (c) (d)

FIGURE 6. ICT images of different bonding layer slice positions.

In order to calculate the depth information of the debonding channel, assume that the fig6 (a) is the initial position and the channel defects appear as shown in fig6 (b) when moving 5.63mm; When the 1.25mm is moved, all the defects appear as shown in fig6(c). When moving 1.25mm, the defect slowly disappears as shown in fig6(d); Through this layered observation of defects, it is clear that the appearance of defects disappears as shown in fig6 (a) and fig6(d). The thickness of the defect at the bonding layer is calculated to be 2.5mm.

Through the analysis of the hole and debonding defects of the above bonding layer, the ICT non-destructive testing technology has a very good detection effect on the interface defects of the new composite bonding layer, and can accurately obtain the parameter information such as the shape, position and type of the defect. Because the defects of composite materials can only be analyzed macroscopically, it is necessary to quantitatively analyze the area and volume of defects in order to analyze the influence of defects on the properties of materials. However, for the void defect of the Fig5(b), we can calculate by the proportional size; For the irregular defect of the Fig6(c), we can't get it by the above method. In order to verify the validity of the proposed method and accurately calculate the area of irregular defects, this paper makes the following analysis.

C. QUANTITATIVE ANALYSIS OF BONDING DEFECTS BASED ON IMAGE SEGMENTATION

The gray-scale slice image with the debonding feature in the main view direction obtained by the ICT scan is selected. It can be seen from the above sliced image that the debonding defect is reduced to disappear from the appearance to the largest area, and debonding defects are irregular. Therefore, the irregular defects bring certain difficulties to the quantitative analysis. In order to accurately calculate the area of debonding defects, we need to verify the effectiveness of the proposed algorithm.

The effect of segmentation algorithm after combining mathematical morphology with FCM algorithm is shown in Fig7. By comparing the FCM algorithm of Fig7(b) with the proposed segmentation algorithm of Fig7(c), it is found that the boundary of the void defect is more clear and the segmentation effect is better. To further validate the method in this paper, we compare the area of the actual void with the method used in this paper. Table4 is a comparison of the

FIGURE 7. Images through the difference segmentation of the sliced images (a) Original image; (b) FCM algorithm segmentation; (c) The algorithm proposed in this paper.

TABLE 4. Defect area of bonding layer.

Figure3 slice diagram	Real area/mm^2	FCM algorithm segmentation area/mm^2	In this paper, algorithm segmentation area/mm^2	error
Figure4（d）	1190.83	1100.36	1149.75	-3.50%
Figure4（e）	2087.28	2160.45	2147.25	+2.87%
Figure4（f）	1770.69	1786.63	1869.75	+5.69%

calculated defect area of the algorithm proposed in this paper and the FCM algorithm. The error between the area obtained by the image segmentation algorithm proposed in this paper and the real defect area is $+2.87\%$, -3.5% and $+5.69\%$, respectively. It can be seen from Table 4 that the algorithm proposed in this paper is better and more accurate than the FCM algorithm in image segmentation.

After many tests data analysis, the measurement error can be controlled at $\pm 6\%$. Therefore, the area of the irregular defect can be estimated, that is, the debonding defect area of the cross channel and the point in Fig6(c) is predicted to be 8636.49mm^2 $\pm$518.19mm^2. Due to the limitation of the resolution of the detection system, the relative error when measuring small adhesion defects is large, and the relative error when measuring large adhesion defects is small. Compared with the normal glue layer boundary, it is closer to the actual shape of the preset defect, and the partially discrete point defects are highlighted, which makes the evaluation of the overall bond quality of the material more accurate.

In order to further accurately study the influence of bonding layer defects on material properties, this article chooses the hole D of the bonding layer in Fig5(b). According to the calculated holes area of each slice, the hole volume is obtained by the accumulation method, that is, according to the idea of three-dimensional segmentation, each slice is regarded as a layer of slices. And the slice area is multiplied by the layer thickness d, where d=0.1mm and the summation is the volume of the hole sought. The formula is as follows

$$\mathrm{V} = \sum_{i=1}^{n} S_i \times d$$

where S_i represents the hole area of $i = 1, 2 \cdot \cdots \cdots n$ slice.

The cumulative method calculates that the volume of the hole is 211.63mm^3. Through the above method, the volume of other holes and the proportion of the defect volume can be calculated. According to the performance index of the safe use of the material, the structural performance of the material can be accurately judged.

According to the distribution characteristics of the gray value of the defects in the ICT tomographic image of the bonding layer, the image segmentation algorithm proposed in this paper is selected to segment the defect, and the defect area can be used to quantitatively calculate the percentage of the defect area in the area of the rubber layer. Combined with the mechanical analysis of the sample, the bonding quality of the aerospace composite can be evaluated.

V. CONCLUSION

Based on ICT technology, it can be visually judged whether the adhesive layer has significant defects; In this paper, a method of combining mathematical morphology with FCM algorithm for accurate detection and characterization of bonding layer defects, has been developed. Then the irregular defect area and volume have been quantified and the error of area range is within $\pm 6\%$. Comparison with the published segmentation algorithm has showed superior performance of proposed method for segment the slice image with the defect region. Therefore, the demand for bonding quality assessment is met and non-destructive testing of bonding defects between composite materials and bonded substrates has been achieved. In the future, we will focus on the quantification and characterization of CT three-dimensional reconstructed images and the evaluation of the bonding quality of bonded structural members, which will provide a strong guarantee for the wide application of new ceramic matrix composites in aerospace.

REFERENCES

[1] N. P. Padture, "Advanced structural ceramics in aerospace propulsion," *Nature Mater.*, vol. 15, no. 8, pp. 804–809, 2016.

[2] L. Kong, X. Zuo, S. Zhu, Z. Li, J. Shi, L. Li, Z. Feng, D. Zhang, D. Deng, and J. Yu, "Novel carbon-poly(silacetylene) composites as advanced thermal protection material in aerospace applications," *Compos. Sci. Technol.*, vol. 162, pp. 163–169, Jul. 2018.

[3] W. Krenkel, "Carbon fibre reinforced silicon carbide composites (C/SiC, C/C-SiC)," in *Handbook of Ceramic Composites*, N. P. Bansal, Ed. Boston,MA, USA: Springer, 2005, pp. 117–148.

[4] D. D. L. Chung, "Carbon fibers, nanofibers, and nanotubes," in *Carbon Composites: Composites With Carbon Fibers, Nanofibers, and Nanotubes*, D. D. L. Chung, Ed. Cambridge, U.K.: Elsevier, 2017, pp. 1–87.

[5] A. Dalmaz, P. Reynaud, D. Rouby, G. Fantozzi, and F. Abbe, "Mechanical behavior and damage development during cyclic fatigue at high-temperature of a 2 · 5D CarbonSiC composite," *Compos. Sci. Technol.* vol. 58, no. 5, pp. 693–699, 1998.

[6] G. Fantozzi and P. Reynaud, "Mechanical behavior of sic fiber-reinforced ceramic matrix composites-2.12," *Comprehensive Hard Materials*, vol. 2014, pp. 345–366.

[7] L. Quemard, F. Rebillat, H. Tawil, C. Louchet-Pouillerie, and A. Guette, "Self-healing mechanisms of a SiC fiber reinforced multi-layered ceramic matrix composite in high pressure steam environments," *J. Eur. Ceramic Soc.*, vol. 27, no. 4, pp. 2085–2094, 2007.

[8] M. Pan, Y. Z. He, G. Y. Tian, D. Chen, and F. Luo, "Defect characterisation using pulsed eddy current thermography under transmission mode and NDT applications," *NDT E Int.*, vol. 52, pp. 28–36, Nov. 2012.

[9] Z. Cai, D. Zou, and C. Liu, "Research on eddy-current testing of functional polymer composite material," *IEEE Trans. Magn.*, vol. 54, no. 11, Nov. 2018, Art. no. 2501005.

[10] R. Raišutis, R. Kažys, E. Žukauskas, and L. Mažeika, "Ultrasonic air-coupled testing of square-shape CFRP composite rods by means of guided waves," *NDT E Int.*, vol. 44, pp. 645–654, Nov. 2011.

[11] E. Jasiūnienė, L. Mažeika, V. Samaitis, V. Cicėnas, and D. Mattsson, "Ultrasonic non-destructive testing of complex titanium/carbon fibre composite joints," *Ultrasonics*, vol. 95, pp. 13–21, May 2019.

[12] N. Chakraborty, V. T. Rathod, D. Roy Mahapatra, and S. Gopalakrishnan, "Guided wave based detection of damage in honeycomb core sandwich structures," *NDT E Int.*, vol. 49, pp. 27–33, Jul. 2012.

[13] Y. Li, A.-B. Ming, H. Mao, G.-F. Jin, Z.-W. Yang, W. Zhang, and S.-Q. Wu, "Detection and characterization of mechanical impact damage within multi-layer carbon fiber reinforced polymer (CFRP) laminate using passive thermography," *IEEE Access*, vol. 7, pp. 27689–27698, 2019.

[14] V. Arora, R. Mulaveesala, A. Sharma, and A. Rani, "Digitised frequency modulated thermal wave imaging for non-destructive testing and evaluation of glass fibre reinforced polymers," *Nondestruct. Test. Eval.*, vol. 34, no. 10, pp. 23–32, 2018.

[15] V. I. Mordasov, N. A. Sazonnikova, N. E. Grebnev, D. N. Grebnev, and A. D. Storozh, "Method of laser vibrating defectoscopy of multilayer composite materials," *Procedia Eng.*, vol. 106, pp. 240–246, Jun. 2015.

[16] Y. Huang, Z. Yang, W. Ren, G. Liu, and C. Zhang, "3D meso-scale fracture modelling and validation of concrete based on *in-situ* X-ray Computed Tomography images using damage plasticity model," *Int. J. Solids Struct.*, pp. 67–68, pp. 340–352, Aug. 2015.

[17] F. Prade, M. Chabior, F. Malm, C. U. Grosse, and F. Pfeiffer, "Observing the setting and hardening of cementitious materials by X-ray dark-field radiography," *Cement Concrete Res.*, vol. 74, pp. 19–25, Apr. 2015.

[18] S. C. Garcea, Y. Wang, and P. J. Withers, "X-ray computed tomography of polymer composites," *Compos. Sci. Technol.*, vol. 156, pp. 305–319, Mar. 2018.

[19] E. Weber, M. Fernandez, W. Hoffman, and P. Wapner, "Comparison of X-ray micro-tomography measurements of densities and porosity principally to values measured by mercury porosimetry for carbon–carbon composites," *Carbon*, vol. 48, no. 8, pp. 2151–2158, 2010.

[20] P. Lall, S. Deshpande, J. Suhling, and J. Wei, "Non-destructive crack and defect detection in SAC solder interconnects using cross-sectioning and X-ray micro-CT," in *Proc. IEEE Electron. Compon. Technol. Conf.*, May 2014, pp. 1449–1456.

[21] A. Perrier, F. Touchard, and L. Chocinski-Arnault, "Quantitative analysis by micro-CT of damage during tensile test in a woven hemp/epoxy composite after water ageing," *Compos. A, Appl. Sci. Manuf.*, vol. 102, no. 11, pp. 18–27, 2017.

[22] Y. Li, B. Sun, and B. Gu, "Impact shear damage characterizations of 3D braided composite with X-ray micro-computed tomography and numerical methodologies," *Compos. Struct.*, vol. 176, no. 9, pp. 43–54, Sep. 2017.

[23] M. Mehdikhani, I. Straumit, L. Gorbatikh, and S. V. Lomov, "Detailed characterization of voids in multidirectional carbon fiber/epoxy composite laminates using X-ray micro-computed tomography," *Compos. A, Appl. Sci. Manuf.*, vol. 125, Oct. 2019, Art. no. 105532.

[24] G. Xue, E. Yilmaz, W. Song, and S. Cao, "Analysis of internal structure behavior of fiber reinforced cement-tailings matrix composites through X-ray computed tomography," *Compos. B, Eng.*, vol. 175, Oct. 2019, Art. no. 107091.

[25] H.-X. Pei, Z.-R. Zheng, C.-N. Li, Y.-H. Shao, and C. Wang, "D-FCM: Density based fuzzy c-means clustering algorithm with application in medical image segmentation," *Procedia Comput. Sci.*, vol. 122, pp. 407–414, 2017.

[26] N. E. A. Khalid, N. M. Noor, and N. M. Ariff, "Fuzzy c-means (FCM) for optic cup and disc segmentation with morphological operation," *Procedia Comput. Sci.*, vol. 42, pp. 255–262, Nov. 2014.

[27] Q. Wang, Q.-P. Zhang, and W. Zhou, "Study on remote sensing image segmentation based on ACA-FCM," *Phys. Procedia*, vol. 33, pp. 1286–1291, Apr. 2012.

[28] S. R. Kannan, S. Ramathilagam, A. Sathya, and R. Devi, "Robust kernel FCM in segmentation of breast medical images," *Expert Syst. Appl.*, vol. 38, no. 4, pp. 4382–4389, 2011.

YINTANG WEN received the B.S. and Ph.D. degrees from the School of Electrical Engineering, Yanshan University, Qinhuangdao, in 1999 and 2018, respectively, where he is currently with the School of Electrical Engineering. His main research interests include intelligent sensing, non-destructive testing and evaluation of advanced composite materials, and health monitoring technology.

SONG ZHANG received the B.S. degree in measurement and control technology and instrumentation from Hebei University, Baoding, in 2017. He is currently pursuing the master's degree in engineering with the School of Electrical Engineering, Yanshan University, Qinhuangdao. His research interests include non-destructive testing technology and image processing.

YUYAN ZHANG received the B.S. and Ph.D. degrees from the School of Electrical Engineering, Yanshan University, Qinhuangdao, in 1999 and 2008, respectively, where she is currently with the School of Electrical Engineering. Her research interests include photoelectric detection technology, non-destructive testing, and structural health monitoring.